Monotonic and cyclic bond behaviour of deformed bars in reinforced concrete structures

G.J. Morris[1], D.K. Bull[1,2] & B.A. Bradley[1]

[1]*Department of Civil and Natural Resources Engineering, University of Canterbury, Christchurch, New Zealand*

[2]*Holmes Consulting Group, New Zealand*

2015 NZSEE Conference

ABSTRACT: A major lesson from the 2011 Christchurch earthquake was the apparent lack of ductility of some lightly reinforced concrete (RC) wall structures. In particular, the structural behaviour of the critical wall in the Gallery Apartments building demonstrated that the inelastic deformation capacity of a structure, as well as potentially brittle failure of the reinforcement, is dependent on the level of bond deterioration between reinforcement and surrounding concrete that occurs under seismic loading. This paper presents the findings of an experimental study on bond behaviour between deformed reinforcing bars and the surrounding concrete. Bond strength and relative bond slip was evaluated using 75 pull-out tests under monotonic and cyclic loading. Variations of the experiments include the loading rate, loading history, concrete strength (25 to 70 MPa), concrete age, cover thickness, bar diameter (16 and 20 mm), embedded length, and the position of the embedded bond region within the specimen (deep within or close to free surface). Select test results are presented with inferred implications for RC structures.

1 INTRODUCTION

Previous seismic experimentation under laboratory conditions has typically shown that RC structural components exhibit a significant spread of plasticity in plastic hinge regions. In contrast, direct observations in the Canterbury earthquake sequence showed lightly reinforced concrete walls may develop a wide single-crack as schematically illustrated in Figure 1. An example of this behaviour was observed in the Gallery Apartments building (Bull 2012). This type of damage mechanism offers limited ductility as the lateral drift of the wall is primarily accommodated by the localised plastic elongation of the vertical reinforcement, resulting in high strain concentrations, and ultimately leading to near or complete brittle fracture of the reinforcement (Canterbury Earthquakes Royal Commission; CERC 2012). This type of damage mechanism also suggests there may have been less extensive bond deterioration compared with the behaviour that occurs in quasi-static testing of RC components (CERC 2012). Practising structural engineers have since been challenged on how to estimate the peak strain demands and available ductility of lightly reinforced wall buildings.

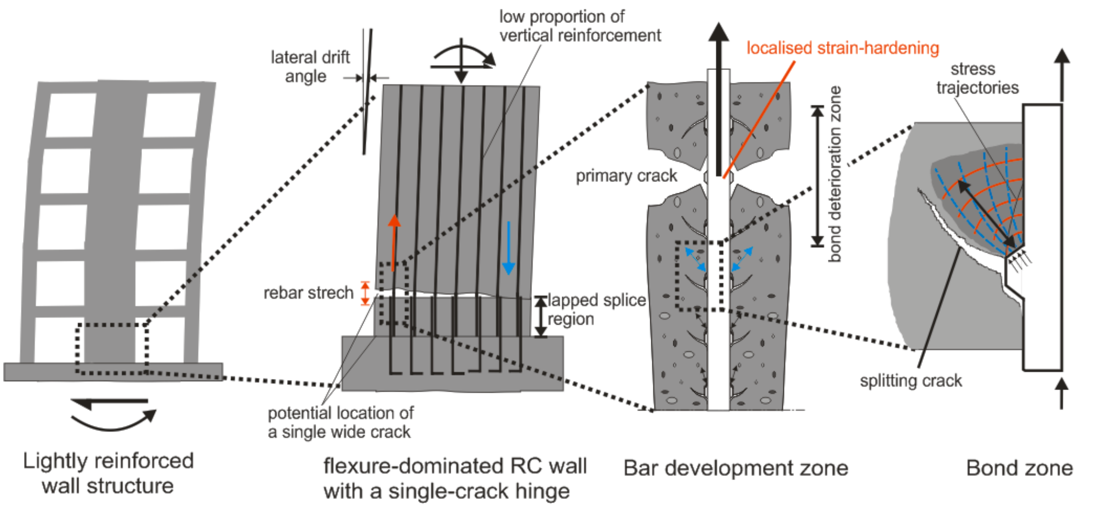

Figure 1. Role of bond behaviour and failure patterns in the overall response of lightly reinforced walls.

There are several potential factors that contributed to the type of damage shown in Figure 1, such as the influence of the rate and sequence of loading, in-place concrete strength, the quantity of vertical reinforcement and the extent of bond deterioration between the vertical reinforcement and surrounding concrete (Henry 2013; Morris et al. 2014). In order to further understand bond mechanics, 75 bond pull-out tests were performed. Different specimens and loading protocols were used to assess the influence of the rate and sequence of loading and the in-place concrete strength. In the following sections the experimental test set-up and specimen details are discussed, followed by an examination of the experimental results and implications for the seismic performance of RC structures.

2 EXPERIMENTAL PROGRAMME

2.1 Pull-out test set-up and specimen particulars

Direct pull-out tests have been commonly used in experimental studies on bond behaviour due to the ease and repeatability of constructing and testing a large number of specimens where a range of parameters can be studied independently. Results from previous bond pull-out tests have also been widely used in the development in constitutive bond stress-slip relationships that have been implemented in the CEB-FIP (now *fib*) Model Codes (1993; 1996; 2012).

Figure 2(a) schematically illustrates the loading frame used to support the relatively massive concrete block as the deformed test bars were connected to a threaded base plate. The top plate provided fixity to a load cell and to the Instron testing machine (load capacity of 100 kN) used to load the test bar. Adjustability of the loading frame was beneficial for minimizing the effect of any accidental eccentricities in the direction of loading applied to the test bar.

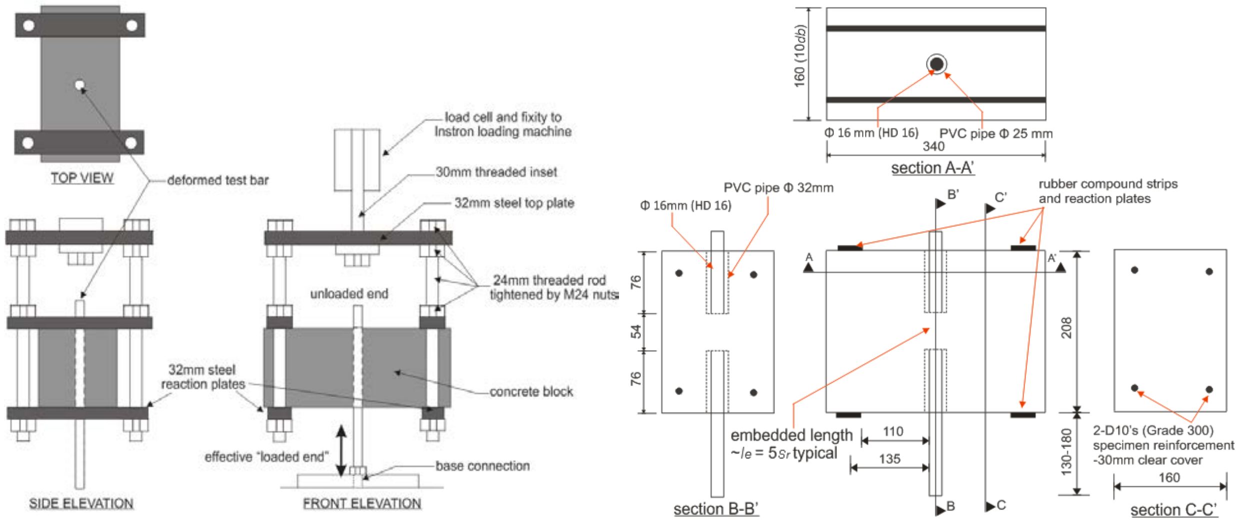

(a) test set-up **(b)** typical specimen details

Figure 2. Illustration of the pull-out test set-up and specimens used to assess local bond behaviour.

Figure 2(b) shows the nominal dimensions of a typical pull-out specimen. A large specimen width was required to ensure that reaction plates were well-spaced in order to mitigate any interference with stresses in the bond zone that may affect the actual bond strength. The loading arrangement meant that specimens would develop some flexural stresses and the specimen design therefore needed to ensure that potential flexural cracking does not drastically affect the bond condition. Specimens typically had a 16 mm deformed test bar (HD16) and a 54 mm embedment length (five times the clear rib spacing). The short embedment length was specifically chosen to ensure that these tests provided some insight to local bond behaviour.

Each concrete pour of 115 litres allowed eight pull-out specimens and nine cylinder samples to be cast. Seven pours had a specified water-cement ratio of 0.57, and two pours targeted 0.44 and 0.74 in attempt to obtain reasonable higher and lower strength variations, respectively. Compressive cylinder test results are presented in last column of Table 1. For the predominant mix, the mean compressive strength was 46 MPa at the time of conducting bond tests (standard deviation of 2.5 MPa).

2.2 Test permutations

Table 1 provides a summary of permutations that were chosen. 47 specimens were subjected to monotonic loading and 28 were subjected to cyclic loading. Before undertaking the entire construction sequence, to gain some initial experience in carrying out testing procedures and observing the specimen behaviour, three "trial specimens" were prepared and tested. Eight "Series" (and Rows within each Series) were established as categories for each permutation. The typical set of "standard" parameters can be deduced from Table 1.

Table 1. Test programme for investigating bond behaviour (excludes three trial tests).

Series	Row	Variable	Type of loading[1]	Slip rate $\dot{s}$ [mm/min]	Bar diameter, d_b [mm]	Design w/c ratio	Bond Length, l_e [mm]	Clear cover [mm]	Number of tests (72)	Actual f'_c [MPa]
1	1	Side cover	3 x MON 1 x LH1	2.0	16	0.57	54	48	4	47.5
	2							96	4	
2	1	Slip rate	3 x MON	100	16	0.57	54	72	3	44.9
	2			2.0					2	
	3			0.1					3	
3	1	Bonded depth from free surface	1 x MON tension 1 x MON compression 2 x LH1	2.0	16	0.57	54	72	4	37.4[2]
	2								4	
	3					0.57			4	41.8
	4								4	
4	1	Loading history	1 MON + 1 LH1	2.0	16	0.57	54	72	2	49.2
	2		3 LH2						3	
	3		3 LH4						3	
5	1	Embedment length	2 x MON 1 x LH1	2.0	16	0.57	87	72	4	43.7
6	1	Bar diameter	2 x MON 1 x LH1	2.0	20		62	72	4	
7	1	Concrete strength	5 x MON 1 x LH1 2 x LH2	2.0	16	0.74	54	72	8	22.5
	2		5 x MON 1 x LH2 2 x LH3			0.44			8	70.8
8	1	Concrete maturity	1 x MON 3 x LH1	2.0	16	0.57	54	72	4	46.3
	2								4	52.7

[1] types of loading protocols and designations described in Section 2.3.

[2] observed to be too wet during mixing and is ignored from statistical comparisons of concrete strength

The influence of loading rate on bond behaviour was studied under monotonic loading only. Other researchers have found that bond strength is enhanced when faster loading rates are applied (Vos and Reinhardt 1982; Eligehausen et al. 1983). However, a large amount of scatter between previous test results has limited attempts to quantify the amount of dynamic influence (Michael and Keuser 2014). The benchmark loading (slip) rate of 2 mm/min was chosen for the reasonable test duration. The speed of the Instron machine governed the maximum and minimum loading rate of 100 mm/min and 0.1 mm/min (50 times faster and 20 times slower than the standard rate, respectively). The fastest and slowest tests were completed within duration of about 15 seconds and 200 minutes, respectively.

2.3 Loading protocols

Monotonic “pull-out” (bar in tension) tests (MON) were performed to provide some benchmark information about the maximum bond resistance. Some monotonic compression “push-in” MON tests were also performed. Cyclic loading was displacement controlled based on measurements of bond slip. The approximate test duration was 10 minutes for monotonic loading and 120 minutes for cyclic loading under LH1, shown in Figure 3(b). LH1 was chosen to be representative of typical gradually increasing loading protocols which are usually fully symmetric for RC components, but not for the flexural reinforcement that is unlikely to undergo full bond slip reversal. Figure 3(c) and 3(d) shows two loading protocols that applied constant slip increments for both fully reversed (LH2) and unidirectional loading (LH3). Figure 3(e) and 3(f) shows LH4 and LH5 that were chosen to represent the bond slip demands for a small number of high amplitude loading cycles.

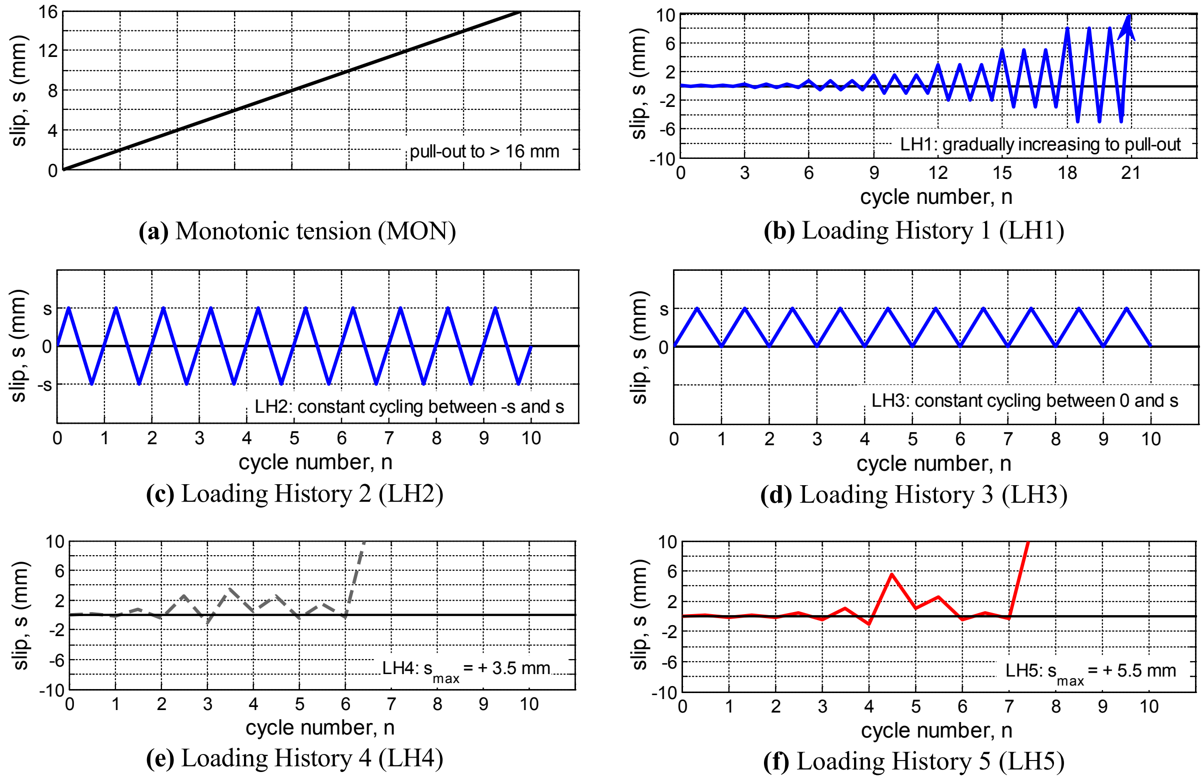

Figure 3. Examples of five loading protocols applied in cyclic bond pull-out testing.

3 EXPERIMENTAL RESULTS AND DISCUSSION

3.1 Observed failure modes

As desired, pull-out failure was the predominant failure mode as the concrete between the ribs is severely crushed and shear cracking occurs when the maximum bond strength is reached. The bond failure surface for a pull-out failure is shown in Figure 4(a). Compacted cement paste and sand particles embedded between the ribs of the test bar is shown in Figure 4(b). Different failure modes observed during monotonic and cyclic testing are quantified in Table 2.

Table 2. Quantity of different failure modes observed during bond pull-out testing.

Failure mode	Monotonic tests	Cyclic tests	Total
Pull-out bond failure	32	21	53
Splitting bond failure	4	3	7
Cone break out failure	3	3	6
Prying failure	8	1	9
Total	47	28	75

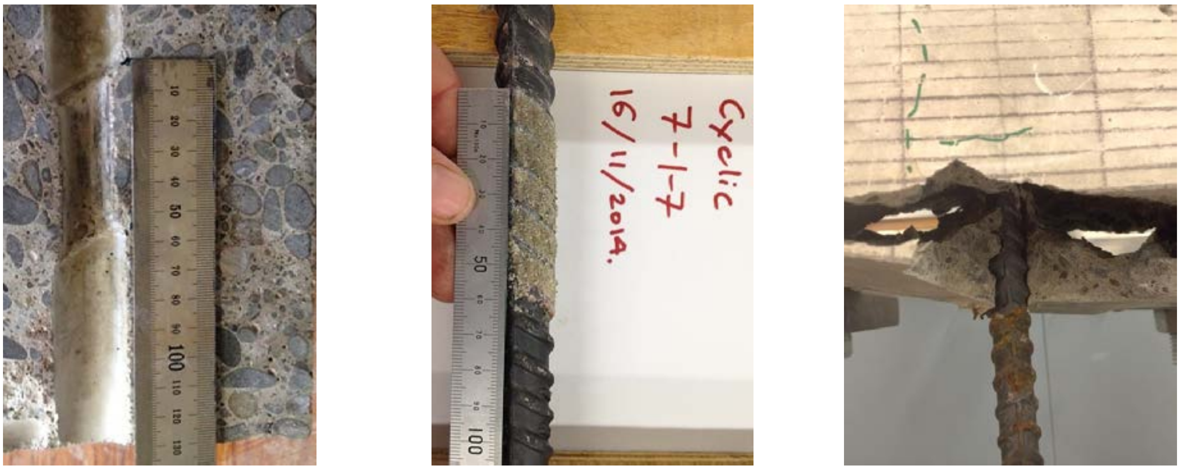

(a) Saw-cut specimen cross section **(b)** HD16 test bar with concrete between ribs **(c)** Cone failure during Test 3-1-1

Figure 4. Photograph of observed pull-out failure in (a) and (b), and cone break-out failure in (c).

Bond "splitting failure" was observed, despite specimens being designed with a reasonable cover thickness with the intention of mitigating this failure mode. Splitting failure occurred in four monotonic tests and in cyclic tests in the slip range between 0.3 and 1.0 mm when high bond stresses developed. Cone break-out failure was observed in Series 3 (at lower bond stresses). Figure 4(c) shows that cone break-out occurs before the concrete between the ribs is severely crushed. Based on measurements, the angle at which the cone broke out was between 25 and 35 degrees.

Unfortunately, premature failure occurred in nine tests due to excessive prying of the specimen. Inspection of the nine damaged specimens found an accidentally large cover thickness to the flexural reinforcement (2-D10s) which meant an excessively large flexural crack was could widen to 3-5 mm. All the deformation was concentrated at the widening of the crack in the mid-span while the concrete either side of the crack behaved like two rigid blocks. Above the neutral axis the compression side of the specimen behaves as a continuous member where the flexural compression force induces large curvature. Premature failure of the specimen is the result of tensile stresses in the transverse direction (across the neutral axis) due to incompatible deformations between the tension and compression regions. The specimen was effectively folding itself around the bond region where additional stresses in the concrete restricted some tests from providing a true representation of the bond behaviour.

3.2 Deducing the bond stress-slip relationship

A fundamental assumption was that the applied loading (measured from the load cell) is equal and opposite to the bond stresses that is assumed to be uniformly distributed over the embedded bond surface area. The values of the average local bond stress, τ, reported in this research have therefore been determined using Equation 1.

$$\tau = \frac{T}{\pi d_b l_e} \qquad \text{[MPa]} \tag{1}$$

where T = applied force [N]; d_b = nominal bar diameter [mm] ; l_e = embedment length [mm]. It was reasonable to assume the bond stress distribution as being uniform as the embedded bond length was relatively short (compared to long anchorage lengths with non-uniform bond stresses). The true definition of local bond slip, $s(x)$, is given by Equation 2.

$$s(x) = \left(\int_{x_0}^{x} \varepsilon_s dx - \int_{x_0}^{x} \varepsilon_c dx\right) + S_0 \tag{2}$$

where S_0 is global slip at the unloaded free-end of the bar, and; the bracketed term refers to the local slip due to relative strain incompatibility between the reinforcing steel ε_s and concrete ε_c from the free end x_0 to a particular position *x*. Since steel strains at the loaded end did not exceed yield during testing, the additional slip due to local bar elongation along such a short embedment length was unlikely to exceed 0.1 mm. It was therefore assumed that the bracketed term in Equation 2 could be neglected and the local bond slip was approximately equal to the free-end slip, i.e. $s(x) \approx S_0$.

3.3 Monotonic test results

47 monotonic bond tests were completed, of these the test bar was predominantly pulled out (bar in tension). Two tests showed the maximum bond stress did not vary significantly when the test bar was pushed in compression for the levels of strain developed in the bars during testing.

Figure 5(a)-(d) present the bond stress-slip relationships deduced from selected tests. In general, the ascending branch shows the initial bond stiffness is very high. Results in Figure 5(a) show that, for a concrete strength of 25 MPa, there is a slight plateau in the maximum bond stress between slip values of 0.8 and 2.0 mm. However, increasing the concrete strength (and hence stiffness) has an influence on both the curvature of the ascending branch in the pre-peak range and the bond behaviour is more "peaked". In the post-peak range the bond stress reduces until the clear rib spacing has been exceeded, as labelled on Figure 5(c). By this stage, the concrete key between the ribs being completely sheared off and mechanical bearing resistance is completely destroyed. Further bond slip has some residual bond stress due to frictional resistance and cement dust was falling out of the specimen.

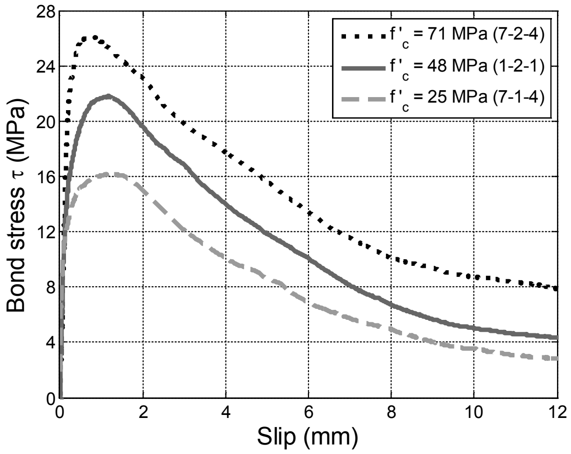

(a) Influence of concrete strength

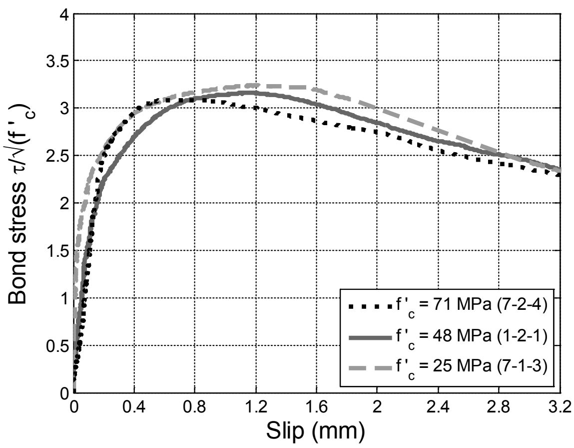

(b) Normalised bond strength in peak range of slip

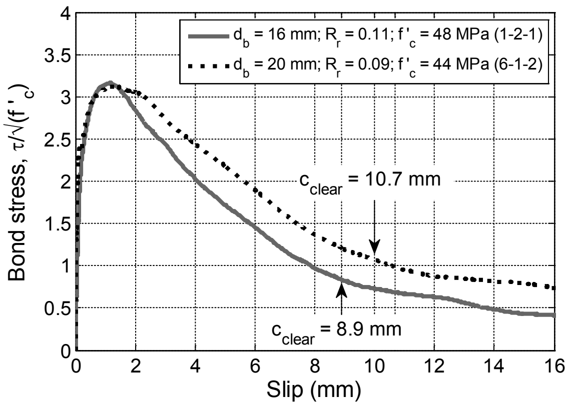

(c) Influence of deformed bar size

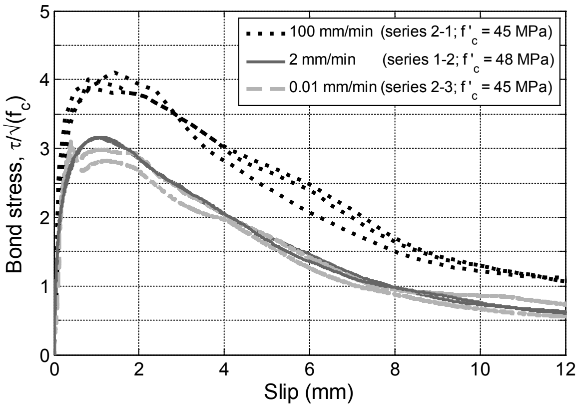

(d) Influence of loading (slip) rate

Figure 5. Monotonic bond stress-slip relationship deduced from bond pull-out tests.

Figure 5(a) illustrates that bond stress is significantly influenced by the concrete strength. Previous researchers (e.g. Eligehausen et al. 1983) and the Model Codes (CEP-FIB, 1993; *fib*, 2012) typically present the maximum local bond stress using a co-efficient k according to Equation 3, where f'_c = concrete compressive strength found from cylinder tests at the time of bond pull-out testing.

$$k = \frac{\tau_{max}}{(f'_c)^{1/2}} \tag{3}$$

The maximum local bond stress considered in the Mode Code 2010 (*fib*, 2012) is given as $2.5(f'_c)^{1/2}$. In general, monotonic test results for pull-out failure had a mean k value of 3.1 and a standard deviation of 0.4. The normalised bond stress in the "peak range" of slip is presented in Figure 5(b). Although a large variation of concrete strengths was used, the normalisation appears reasonable for this study. Some minor variation between the normalised bond stress-slip curves is expected due to inherent variability of the mechanical properties of concrete.

Figure 5(c) illustrates that bar size has some effect on the point at which bond stress is solely attributed to friction along the bond surface. Compared with the HD16 bars, the HD20 bar has a slightly larger rib spacing (8.9 and 10.7 mm, respectively) which means there is a longer concrete key to provide mechanical bearing resistance for slightly larger slip values.

Figure 5(d) shows that increasing the loading (slip) rate by a factor of 50 corresponds to an increased maximum bond stress of approximately 30%, while decreasing the loading rate by a factor of 20 suggested the static bond strength may be 10% less. These results suggest it was reasonable to adopt a slip rate equal to 2 mm/min as the standard slip rate for other tests. Other attempts to quantify dynamic influence factors on bond strength have found significant scatter between test results (Michal and Keuser 2014). Given the number of tests that were performed specifically for Series 2, it is inappropriate to directly adopt these results as the dynamically-enhanced bond behaviour.

3.4 Cyclic test results

As previously mentioned, 28 cyclic bond tests were performed using five different cyclic loading protocols. Figure 6(a) presents the typical behaviour during the loading protocol LH1. In general, the bond strength and stiffness on the first cycle in compression was either the same or of lower amplitude than the previous cycle in tension. No tests showed greater bond resistance in the negative direction, which was anticipated due to the concrete casting direction (Park and Paulay 1975).

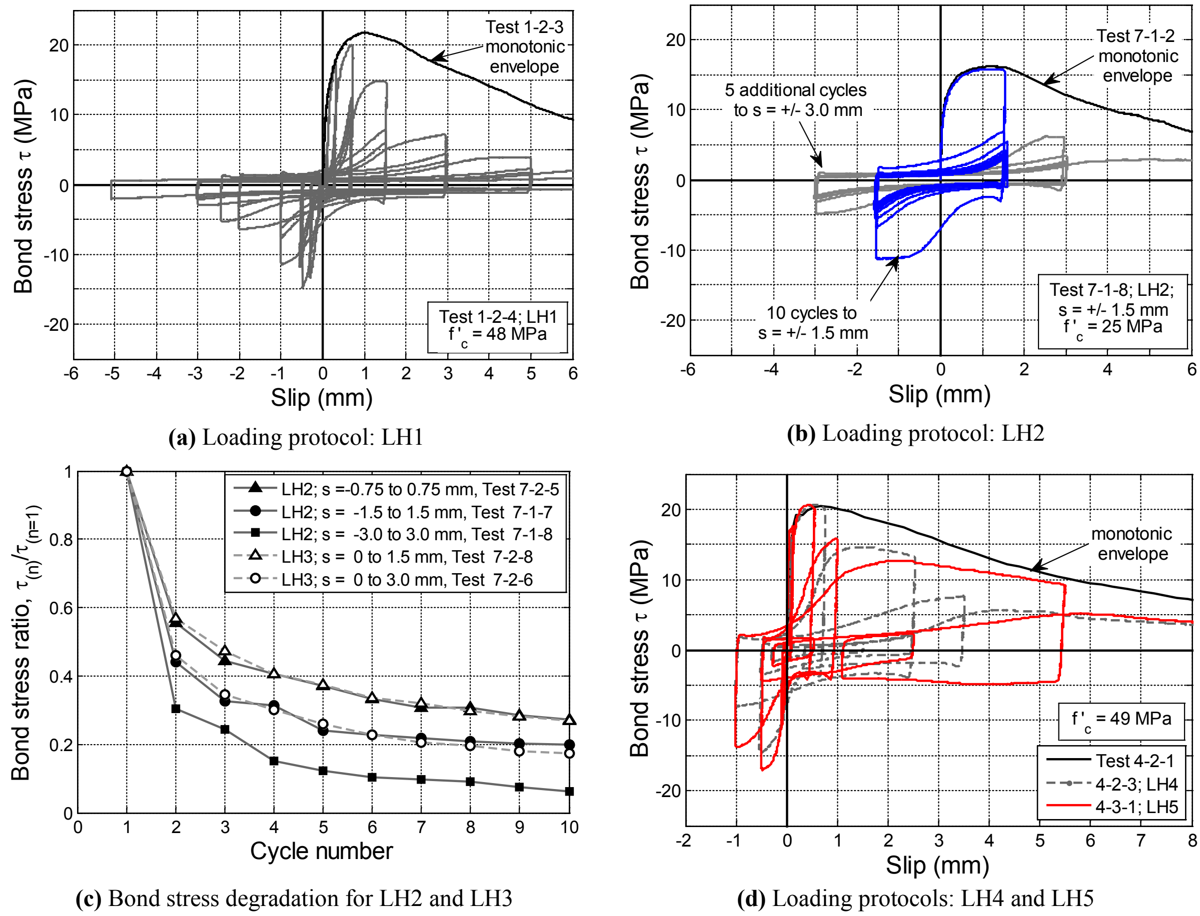

(a) Loading protocol: LH1

(b) Loading protocol: LH2

(c) Bond stress degradation for LH2 and LH3

(d) Loading protocols: LH4 and LH5

Figure 6. Cyclic bond behaviour deduced from bond pull-out tests.

Figure 6(a) and (b) show that, if bond slip is greater than previously sustained, the bond-stress slip curves are shown to be is concave on the first cycle and re-loading cycles to the same slip does not mobilise any additional bearing resistance. Instead, the damaged concrete in the vicinity of the ribs is cracked and crushed and bond slip is irrecoverable. Reloading to the onset of newly mobilised mechanical bearing is shown by a point of inflexion in the bond stress-slip curve. During cyclic loading, mechanical bearing is destroyed once the slip range is equal to the clear rib spacing, as shown by the cycles between -3.0 mm and 5.0 mm on Figure 6(a).

Constant slip amplitudes were applied in LH2 for fully reversed loading cycles, as shown in Figure 6(b), and in LH3 for half cycles of unidirectional loading. Bond stress degradation for 10 loading cycles to different slip amplitudes is presented in Figure 6(c). In general, all tests showed significant damage occurs in the first loading cycle and the majority of the damage occurs in the first five loading cycles. Figure 6(c) also shows the bond strength degradation is approximately the same for loading with full and half cycles with two identical slip ranges of 1.5 mm and 3.0 mm.

A smaller number of high amplitude loading cycles were applied in two loading protocols LH4 and LH5 that were used as a crude representation of the response history induced by the 22 February 2011 Christchurch earthquake. Figure 6(d) shows the post-peak bond stress at +2.0 mm slip is about 2.5 times greater than that in Figure 6(a). Cyclic bond behaviour is shown to be significantly influenced by the number and amplitude of loading cycles.

4 CONCLUSIONS AND IMPLICATIONS OF THIS RESEARCH

This paper briefly outlined the experimental programme that was established for the purposes of evaluating different tests parameters on both monotonic and cyclic bond behaviour. A simple and repeatable test set-up was designed and 75 pull-out specimens were constructed and tested in order to deduce the bond stress-slip relationship. Select test results and preliminary discussion for monotonic and cyclic behaviour was presented in this paper following the recent completion of some experimental testing programme.

On average, monotonic tests showed the maximum local bond stress was generally higher than values stated in the Model Code 20120 (*fib* 2012). Increasing the concrete strength in one series, and loading rate in another series, showed an enhanced the bond resistance. Cyclic tests with different loading protocols showed the post-peak bond strength depends on the bond slip range and the number of cycles. Gradually increasing fully-reversed loading protocols cause relatively extensive bond deterioration compared to loading protocols with a small number of large amplitude cycles.

Certain in-situ conditions, such as lightly reinforced wall structures with moderate to high concrete strengths, very high bond stresses may be mobilised by a relatively small amount of bond slip during short duration pulse-like loading. The ultimate concern with these findings is that such high bond resistance may lead to non-conservative assumptions or predictions of the maximum crack width and/or length that the vertical reinforcement has yielded over, thus leading to over-estimates in the potential ductility of lightly reinforced structural components.

5 ACKNOWLEDGEMENTS

The opportunity to undertake this research was made possible by the financial support from the University of Canterbury (UC), the UC Quake Centre, and the SAFER Concrete Technology project funded by the Ministry of Business, Innovation and Employment (MBIE) via the Natural Hazards Research Platform. Advice provided by Professor Richard Fenwick is greatly appreciated. Support from technical staff at UC and cement donated by Holcim were invaluable to this research.

6 REFERENCES

Bull, D.K. 2012. The performance of concrete structures in the Canterbury earthquakes: Lessons for concrete buildings, *Structural Engineers Association of California (SEAOC) Convention*, Santa Fe, NM.

Canterbury Earthquakes Royal Commission, CERC 2012. Final report: Volume 2, The performance of Christchurch CBD Buildings.

Comite' Euro-internationale du beton (CEB-FIP, 1993). The Model Code 1990: *Design code*. London: T. Telford; 1993.

Eligehausen, R., Popov, E.P., Bertero, V.V. 1983. Local bond stress-slip relationships of deformed bars under generalized excitations. *Report UCB/EERC-83/23,* University of California, Berkeley.

Fédération Internationale du Béton (*fib*, 2012). Model Code 2010 - Final draft, Volume 2. fib Bulletin No. 66, Lausanne, Switzerland.

Henry, R.S. 2013. Assessment of minimum vertical reinforcement limits for RC walls, *Bulletin of the New Zealand Society for Earthquake Engineering*, 46(2): 88-96.

Michael, M. & Keuser, M. 2014. Bond of steel and concrete under high loading rates. *Proceedings of the 9th International Conference on Structural Dynamics*, Porto, Portugal.

Morris, G.J., Bull, D.K. & Bradley, B.A. (2014. Reviewing uncertainties in seismic experimentation following the unexpected performance of RC structures in the 2010-2011 Canterbury earthquakes, *Conference proceedings of the NZSEE, March 2014*, Auckland, New Zealand.

Park, R. & Paulay, T. 1975. Reinforced concrete structures, John Wiley & Son, Inc., New York, United States of America.

Vos, E. & Reinhardt, H.W. 1982. Influence of loading rate on bond behaviour of reinforcing steel and prestressing strands, *Materials and Structures*. RILEM 15(85): 3-10.